

Density Functional Study on the Regioselectivity of Nucleophilic Attack in 1,3-Disubstituted (Diphosphino)(η^3 -allyl)palladium Cations

Vicenç Branchadell,* Marcial Moreno-Mañas,* Francesca Pajuelo, and Roser Pleixats

Department of Chemistry, Universitat Autònoma de Barcelona, Cerdanyola, 08193-Barcelona, Spain

Received May 18, 1999

A density functional study has been performed to analyze the influence of electronic effects on the regioselectivity of the Tsuji–Trost reaction. Optimized geometries of model (diphosphino)(η^3 -allyl)palladium cations **6** and **7** show that for unsymmetrical allyl ligands the shortest Pd–C(terminal) bond is the one closest to the most electron-withdrawing group. The calculated energy barriers for the attack of an ammonia molecule at each one of the terminal allyl carbon atoms of **7b–d** predict that nucleophilic attack would take place preferentially on the carbon atom remote from the most electron-withdrawing group, in excellent agreement with experimental observations on allylic precursors of cations **4**.

Introduction

The palladium(0)-catalyzed allylation of nucleophiles (the Tsuji–Trost reaction) is a synthetic method widely accepted due to its broad applicability and facile experimental procedure.¹ The catalytic cycle (Figure 1) requires the formation of the (η^3 -allyl)palladium(II) complex **1**, an intermediate which can be attacked by nucleophiles at both termini of the allylic system. It is generally accepted that nucleophiles attack preferentially the less hindered allylic terminus, product **2** thus being predominantly formed, mainly if R = alkyl, aryl. However, the situation is not so simple. Thus, for a given nucleophile the regioselectivity depends on the electronic nature of the ligand L, acceptor ligands favoring attack at the more substituted terminus;² and for a given allylpalladium system regioselectivity can depend on the nucleophile, nonstabilized nucleophiles presenting some propensity for attack at the more substituted terminus.³ Electronic effects are superimposed with steric effects mainly when R in Figure 1 is a polar group. Thus, electron-withdrawing groups (positive σ_p values) direct the attack on complexes **1** at the more remote side

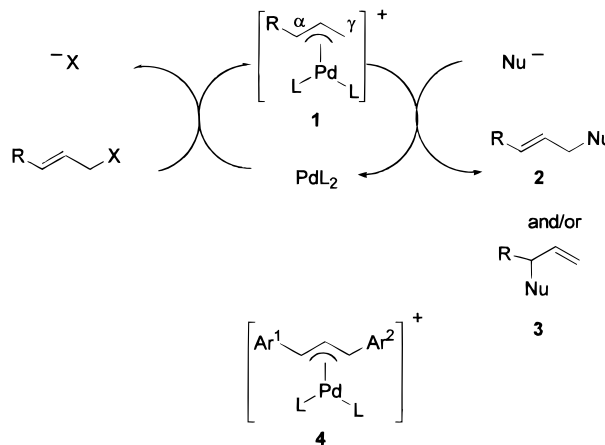


Figure 1. Catalytic cycle for the Tsuji–Trost reaction: intermediate (diphosphino)(η^3 -1,3-diarylallyl)palladium cations **4**.

(γ attack: R'CO– and R'OCO–,⁴ NC–,^{4d,e,5} PhSO₂–,⁶ (R'O)₂P(O)–,⁷ PhS–⁸), whereas electron-donating groups favor the attack at the same position (α attack: R'O–,⁹

(1) For reviews see: (a) Trost, B. M.; Verhoeven, T. R. *Organopalladium Compounds in Organic Synthesis and in Catalysis*. In *Comprehensive Organometallic Chemistry*; Wilkinson, G., Stone, F. G. A., Abel, E. W., Eds.; Pergamon Press: New York, 1982; Vol. 8, Chapter 57. (b) Trost, B. M. *Acc. Chem. Res.* **1980**, *13*, 385. (c) Trost, B. M. *Chemtracts-Org. Chem.* **1988**, *1*, 415. (d) Trost, B. M. *Angew. Chem., Int. Ed. Engl.* **1989**, *28*, 1173. (e) Godleski, S. A. Nucleophiles with Allyl-Metal Complexes. In *Comprehensive Organic Synthesis*; Trost, B. M., Fleming, I., Eds.; Pergamon Press: New York, 1991; Vol. 4, Chapter 3.3. (f) Tsuji, J.; Minami, I. *Acc. Chem. Res.* **1987**, *20*, 140. (g) Tsuji, J. *Tetrahedron* **1986**, *42*, 4361. (h) Heck, R. F. *Palladium Reagents in Organic Synthesis*; Academic Press: London, 1985. (i) Consiglio, G.; Waymouth, R. M. *Chem. Rev.* **1989**, *89*, 257. (j) Frost, C. G.; Howarth, J.; Williams, J. M. J. *Tetrahedron: Asymmetry* **1992**, *3*, 1089. (k) Tsuji, J. *Palladium Reagents and Catalysts*; Wiley: Chichester, U.K., 1995. (l) Harrington, P. J. Transition Metal Allyl Complexes: Pd, W, Mo-assisted Nucleophilic Attack. In *Comprehensive Organometallic Chemistry II*; Abel, E. W., Stone, F. G. A., Wilkinson, G., Eds.; Pergamon Press: New York, 1995; Vol. 12, Chapter 8.2. (m) Moreno-Mañas, M.; Pleixats, R. *Adv. Heterocycl. Chem.* **1996**, *96*, 73.

(2) (a) Trost, B. M.; Strege, P. E. *J. Am. Chem. Soc.* **1975**, *97*, 2534. (b) Trost, B. M.; Weber, L.; Strege, P. E.; Fullerton, T. J.; Dietsche, T. *J. Am. Chem. Soc.* **1978**, *100*, 3416. (c) Åkermark, B.; Hansson, S.; Krakenberger, B.; Vitagliano, A.; Zetterberg, K. *Organometallics* **1984**, *3*, 679. (d) Cuvigny, T.; Julia, M.; Rolando, C. *J. Organomet. Chem.* **1985**, *285*, 395. (e) Åkermark, B.; Vitagliano, A. *Organometallics* **1985**, *4*, 1275. (f) Åkermark, B.; Zetterberg, K.; Hansson, S.; Krakenberger, B.; Vitagliano, A. *J. Organomet. Chem.* **1987**, *335*, 133. (g) von Matt, P.; Lloyd-Jones, G. C.; Minidis, A. B. E.; Pfaltz, A.; Macko, L.; Neuburger, M.; Zehnder, M.; Rüegger, H.; Pregosin, P. S. *Helv. Chim. Acta* **1995**, *78*, 265. (h) Pregosin, P. S.; Salzmänn, R. *Coord. Chem. Rev.* **1996**, *155*, 35. (3) Keinan, E.; Sahai, M. *J. Chem. Soc., Chem. Commun.* **1984**, 648. (4) (a) Jackson, W. R.; Strauss, J. U. G. *Tetrahedron Lett.* **1975**, 2591. (b) Collins, D. J.; Jackson, W. R.; Timms, R. N. *Tetrahedron Lett.* **1976**, 495. (c) Jackson, W. R.; Strauss, J. U. *Aust. J. Chem.* **1977**, *30*, 553. (d) Tsuji, J.; Ueno, H.; Kobayashi, Y.; Okumoto, H. *Tetrahedron Lett.* **1981**, *22*, 2573. (e) Ognyanov, V. I.; Hesse, M. *Synthesis* **1985**, 645. (f) Ono, N.; Hamamoto, I.; Kaji, A. *J. Chem. Soc., Perkin Trans. 1* **1986**, 1439. (g) Tanikaga, R.; Jun, T. X.; Kaji, A. *J. Chem. Soc., Perkin Trans. 1* **1990**, 1185. (5) Keinan, E.; Roth, Z. *J. Org. Chem.* **1983**, *48*, 1769.

anomeric oxygen atom in unsaturated carbohydrates¹⁰. The influence of other groups has been also described: in general the acetoxy group (MeCOO⁻) induces α attack,¹¹ although steric effects can reverse this propensity;^{11a,b,d,12} the regioselectivity for R = fluorine depends on the nature of the nucleophile;¹³ the trimethylsilyl group clearly induces γ attack,^{14,15} although it is neither electron-withdrawing nor electron-donating (σ_p in the range 0.00 to -0.07), and the same applies to the tributyltin group.¹⁵ Therefore, other reasons should be invoked to explain regioselectivity induced by these group 14 elements.

To make clear the role of electronic effects on the regioselectivity in the absence of any steric interference, some of us have studied Pd(0)-catalyzed allylations of soft nucleophiles with 1,3-diarylallyl systems.¹⁶ These reactions involve the (η^3 -allyl)palladium complexes **4** (L/L = PPh₃/PPh₃ or Ph₂PCH₂CH₂PPh₂) featuring para-substituted aryl rings (Figure 1) that confer equal steric requirements but different electronic requirements at both ends of the allylic system. Complexes **4** (Ar¹ = 4-CiPh, 4-MeOPh, Ar² = 4-NO₂Ph;^{16a} Ar¹ = Ph, Ar² = 4-MeOPh^{16b}) were studied, and the experimental conclusion is clear: the nucleophilic attack takes place preferentially at the terminus remote from the most electron-withdrawing group.¹⁶

For a better understanding of this clear experimental tendency, we prepared the (1,2-bis(diphenylphosphino)ethane)(η^3 -1,3-diarylallyl)palladium tetrafluoroborates **5** (Figure 2) and found that the ¹³C NMR chemical shifts of C-1 and C-3 correlate well with σ_p Hammett constants of the substituents at the aryl rings (Figure 2).^{16b} Of course, NMR studies require independent preparation of (η^3 -allyl)palladium salts, but these intermediate complexes are not isolated when performing Tsuji–Trost chemistry. Therefore, Hammett substituent constants are valuable indicators to anticipate the site of

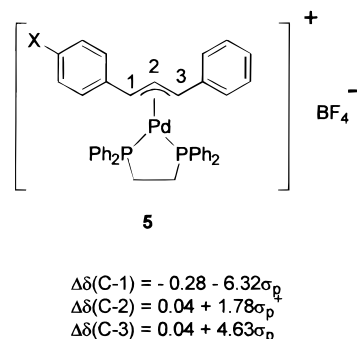


Figure 2. (1,2-Bis(diphenylphosphino)ethane)(η^3 -1,3-diarylallyl)palladium tetrafluoroborates **5**.

attack by soft nucleophiles. Some features of the correlations are noteworthy. Thus, the chemical shift of C-1 is displaced at higher field by electron-withdrawing substituents, whereas the chemical shifts of C-2 and C-3 are displaced at lower fields by the same substituents. The negative sign of the C-1 correlation is against intuition, although this type of behavior is not uncommon in organometallic chemistry^{17,18} and, in particular, in related (η^3 -allyl)palladium complexes.¹⁹ In fact, concerning prediction of regioselectivity, the conclusion is that for each complex the chemical shift at lower field indicates the site (C-1 or C-3) of preferred attack by soft nucleophiles in the Tsuji–Trost reaction. Moreover, $\Delta\delta$ for C-1 and for C-3 correlate well with the σ_p substituent constants but, in contrast, $\Delta\delta$ for C-2 correlates much better with σ_p^+ . These correlation data, together with the much lower field chemical shifts of the signals of C-2 carbon atoms, point out a concentration of positive charge at C-2. In fact, Pd-catalyzed attacks at C-2 by hard nucleophiles to afford cyclopropyl derivatives are well-established for substituted allyl systems in general²⁰ and for the 1,3-diphenyl system in particular.^{20c,e} However, soft nucleophiles attack at the terminal carbon atoms of the allylic system when the palladium is stabilized by phosphines.^{20e}

Theoretical calculations have been performed on (η^3 -allyl)palladium complexes dealing with diverse aspects of the complexes. The nucleophilic attack on allylpalladium complexes was first studied by Sakaki et al.,²¹ who analyzed the role of ancillary ligands by means of semiempirical CNDO calculations. Later, the same author²² performed theoretical calculations on geometries, bonding nature, and relative stabilities of dinuclear palladium(I) η^3 -allyl complexes and mononu-

(6) (a) Ogura, K.; Shibuya, N.; Iida, H. *Tetrahedron Lett.* **1981**, *22*, 1519. (b) Alonso, I.; Carretero, J. C.; Garrido, J. L.; Magro, V.; Pedregal, C. *J. Org. Chem.* **1997**, *62*, 5682.

(7) (a) Zhu, J.; Lu, X. *Tetrahedron Lett.* **1987**, *28*, 1897. (b) Öhler, E.; Kanzler, S. *Synthesis* **1995**, 539. (c) Principato, B.; Maffei, M.; Siv, C.; Buono, G.; Peiffer, G. *Tetrahedron* **1996**, *52*, 2087.

(8) (a) Godleski, S. A.; Villhauer, E. B. *J. Org. Chem.* **1984**, *49*, 2246. (b) Godleski, S. A.; Villhauer, E. B. *J. Org. Chem.* **1986**, *51*, 486. (c) Yamamoto, Y.; Al-Masum, M.; Takeda, A. *J. Chem. Soc., Chem. Commun.* **1996**, 831.

(9) (a) Billups, W. E.; Erkes, R. S.; Reed, L. E. *Synth. Commun.* **1980**, *10*, 147. (b) Trost, B. M.; Merlic, C. A. *J. Org. Chem.* **1990**, *55*, 1127. (c) Chaptal, N.; Colovray-Gotteland, V.; Grandjean, C.; Cazes, B.; Goré, J. *Tetrahedron Lett.* **1991**, *32*, 1795. (d) Vicart, N.; Cazes, B.; Goré, J. *Tetrahedron Lett.* **1995**, *36*, 535. (e) Yamamoto, Y.; Al-Masum, M. *Synlett* **1995**, 969.

(10) (a) Brakta, M.; Lhoste, P.; Sinou, D. *J. Org. Chem.* **1989**, *54*, 1890. (b) Moineau, C.; Bollitt, V.; Sinou, D. *J. Chem. Soc., Chem. Commun.* **1995**, 1103.

(11) (a) Lu, X.; Huang, Y. *J. Organomet. Chem.* **1984**, *268*, 185. (b) Trost, B. M.; Vercauteren, J. *Tetrahedron Lett.* **1985**, *26*, 131. (c) Genét, J.-P.; Uziel, J.; Juge, S. *Tetrahedron Lett.* **1988**, *29*, 4559. (d) Trost, B. M.; Lee, C. B.; Weiss, J. M. *J. Am. Chem. Soc.* **1995**, *117*, 7247.

(12) Sjögren, M. P. T.; Hansson, S.; Åkermark, B.; Vitagliano, A. *Organometallics* **1994**, *13*, 1963.

(13) Shi, G.; Huang, X.; Zhang, F.-J. *Tetrahedron Lett.* **1995**, *36*, 6305.

(14) (a) Falck-Pedersen, M. L.; Benneche, T.; Undheim, K. *Acta Chem. Scand.* **1989**, *43*, 251. (b) Urabe, H.; Inami, H.; Sato, F. *J. Chem. Soc., Chem. Commun.* **1993**, 1595. (c) Inami, H.; Ito, T.; Urabe, H.; Sato, F. *Tetrahedron Lett.* **1993**, *34*, 5919. (d) Ollivier, J.; Salaün, J. *Synlett* **1994**, 949.

(15) Falck-Pedersen, M. L.; Benneche, T.; Undheim, K. *Acta Chem. Scand.* **1992**, *46*, 1215.

(16) (a) Prat, M.; Ribas, J.; Moreno-Mañas, M. *Tetrahedron* **1992**, *48*, 1695. (b) Moreno-Mañas, M.; Pajuelo, F.; Parella, T.; Pleixats, R. *Organometallics* **1997**, *16*, 205.

(17) For a review of Hammett correlations in organometallic chemistry see: Senoff, C. V. *Coord. Chem. Rev.* **1980**, *32*, 111.

(18) (a) Bitterwolf, T. E. *Polyhedron* **1988**, *7*, 1377. (b) Blais, M. S.; Rausch, M. D. *Organometallics* **1994**, *13*, 3557.

(19) (a) Malet, R.; Moreno-Mañas, M.; Parella, T.; Pleixats, R. *Organometallics* **1995**, *14*, 2463. (b) Malet, R.; Moreno-Mañas, M.; Parella, T.; Pleixats, R. *J. Org. Chem.* **1996**, *61*, 758.

(20) (a) Carfagna, C.; Mariani, L.; Musco, A.; Sallase, G. *J. Org. Chem.* **1991**, *56*, 3924. (b) Hoffmann, H. M. R.; Otte, A. R.; Wilde, A. *Angew. Chem., Int. Ed. Engl.* **1992**, *31*, 234. (c) Otte, A. R.; Wilde, A.; Hoffmann, H. M. R. *Angew. Chem., Int. Ed. Engl.* **1994**, *33*, 1280. (d) Ohe, K.; Matsuda, H.; Morimoto, T.; Ogoshi, S.; Chatani, N.; Murai, S. *J. Am. Chem. Soc.* **1994**, *116*, 4125. (e) Hoffmann, H. M. R.; Otte, A. R.; Wilde, A.; Menzer, S.; Willimas, D. *J. Angew. Chem., Int. Ed. Engl.* **1995**, *34*, 100. (f) Castaño, A. M.; Aranyos, A.; Szabó, K. J.; Bäckvall, J.-E. *Angew. Chem., Int. Ed. Engl.* **1995**, *34*, 2551.

(21) Sakaki, S.; Nishikawa, M.; Ohyoshi, A. *J. Am. Chem. Soc.* **1980**, *102*, 4062.

(22) Sakaki, S.; Takeuchi, K.; Sugimoto, M.; Kurosawa, H. *Organometallics* **1997**, *16*, 2995.

clear palladium(II) η^3 -allyl complexes. Blöchl and Togni²³ have studied the site selectivity for nucleophilic attack at an allylpalladium complex with a bidentate phosphine–pyrazole ligand, observing a strong *trans* influence of the phosphine ligand governing the selectivity. Similar results were obtained by Ward²⁴ on a theoretical study of the regioselectivity of nucleophilic attack on [Pd(allyl)(phosphine)(imine)] complexes. The steric influences on the selectivity in palladium-catalyzed allylations have been analyzed by Norrby et al.²⁵ by correlation of experimental selectivities with steric factors calculated using molecular mechanics. Bäckvall et al.²⁶ have studied theoretically and experimentally the central versus terminal attack in nucleophilic addition to (η^3 -allyl)palladium complexes and have found that both the nature of the nucleophile and the ancillary ligands play an important role in the regiochemistry. In a related work, Szabó²⁷ has investigated the effects of ancillary ligands on palladium–carbon bonding in these types of complexes and their implications on the reactivity and regioselectivity. The same author²⁸ has analyzed the nature of the interactions between β -substituents and the metal atom in (η^3 -allyl)palladium complexes and has discussed the β -substituent effects on the stability of the complexes and on the regioselectivity of nucleophilic addition reactions.

As suitable crystals for X-ray determination of isolated complexes **5** could not be obtained (anions other than tetrafluoroborate were also assayed, such as trifluoromethanesulfonate, tetraphenylborate, and hexafluorophosphate), we decided to undertake a theoretical study to find the optimized geometric parameters for model η^3 -allyl cations. We wanted also to analyze the influence of electronic effects on the regioselectivity of the allylation reaction in order to explain the experimental regioselectivities observed in the reactions having type **4** intermediate cations.

Computational Methods

All the calculations have been carried out by using density functional methods. The molecular geometries have been optimized using the method developed by Versluis and Ziegler²⁹ implemented in the ADF program.³⁰ In these calculations the local density approximation (LDA)³¹ has been used, with the parametrization of Vosko et al.³² The inner shells of C, N, O, P, and Pd have been treated by the frozen core approximation.^{30b} For Pd the core includes up to the 3d shell. For the representation of the valence shells of C, N, O, and P we have used an uncontracted double- ξ basis set of Slater orbitals (STO) augmented with a set of 3d polarization functions. For

H we have used a double- ξ basis set. Finally, for Pd we have used a triple- ξ basis set.³³

Molecular energies have been computed for the LDA-optimized geometries using the hybrid Becke exchange functional³⁴ and the correlation functional of Lee, Yang, and Parr³⁵ (B3LYP) implemented in the Gaussian-98 program.³⁶ In these calculations we have used the effective core potentials of Hay and Wadt for Pd³⁷ and P.³⁸ The valence basis set for Pd has been supplemented with a set of diffuse d functions of exponent 0.0628. For P a set of 3d polarization functions ($\alpha = 0.55$) has been included. For C, N, and O a double- ξ basis set has been used³⁹ supplemented by 3d polarization functions with exponents 0.75, 0.80, and 0.85, respectively. Finally, for H we have used a double- ξ basis set.³⁹

The charge distribution in the complexes has been analyzed from the natural atomic orbital scheme developed by Weinhold et al.⁴⁰ These orbitals are those which diagonalize the block of the density matrix that contains the basis functions belonging to a specific atom. Atomic populations obtained from this analysis are less basis set dependent than those corresponding to the Mulliken population analysis.

¹³C NMR chemical shifts have been computed at the B3LYP level of calculation using the gauge independent atomic orbital (GIAO) method.⁴¹ The GIAO method has already been tested in the calculation of ¹³C NMR chemical shifts in density functional calculations of transition-metal complexes.⁴²

Results and Discussion

Figure 3 represents the structure of the model allylpalladium and 1,3-diaryllallylpalladium complexes **6a–c** and **7a–d** that we have chosen for the theoretical study. Triphenylphosphine ligands have been replaced by PH₃ in order to simplify calculations. The most important optimized geometry parameters are presented in Table 1. We can observe that, in most cases, the distance between Pd and C2 is shorter than those corresponding to the terminal allyl carbon atoms, C1 and C3. For **6a** we have also optimized the geometry at the B3LYP level, obtaining a value of 2.23 Å for both Pd–C1 and Pd–C2. These results can be compared with those obtained at the MP2 level by Szabó²⁷ and Sakaki:²² 2.20–2.21 Å for Pd–C1 and 2.19 Å for Pd–C2.

The presence of a substituent directly bonded to one of the allyl carbon atoms produces an asymmetry in the

(33) Vernooijs, P.; Snijders, G. J.; Baerends, E. J. *Slater Type Basis Functions for the Whole Periodic System*; Internal Report; Freie Universiteit Amsterdam, Amsterdam, The Netherlands, 1981.

(34) Becke, A. D. *J. Chem. Phys.* **1993**, *98*, 1372.

(35) Lee, C.; Yang, W.; Parr, R. G. *Phys. Rev.* **1988**, *A37*, 785.

(36) Frisch, M. J.; Trucks, G. W.; Schlegel, H. B.; Scuseria, G. E.; Robb, M. A.; Cheeseman, J. R.; Zakrzewski, V. G.; Montgomery, J. A., Jr.; Stratmann, R. E.; Burant, J. C.; Dapprich, S.; Millam, J. M.; Daniels, A. D.; Kudin, K. N.; Strain, M. C.; Farkas, O.; Tomasi, J.; Barone, V.; Cossi, M.; Cammi, R.; Mennucci, B.; Pomelli, C.; Adamo, C.; Clifford, S.; Ochterski, J.; Petersson, G. A.; Ayala, P. Y.; Cui, Q.; Morokuma, K.; Malick, D. K.; Rabuck, A. D.; Raghavachari, K.; Foresman, J. B.; Cioslowski, J.; Ortiz, J. V.; Stefanov, B. B.; Liu, G.; Liashenko, A.; Piskorz, P.; Komaromi, I.; Gomperts, R.; Martin, R. L.; Fox, D. J.; Keith, T.; Al-Laham, M. A.; Peng, C. Y.; Nanayakkara, A.; Gonzalez, C.; Challacombe, M.; Gill, P. M. W.; Johnson, B.; Chen, W.; Wong, M. W.; Andres, J. L.; Gonzalez, C.; Head-Gordon, M.; Replogle, E. S.; Pople, J. A. *Gaussian 98, Revision A.5*; Gaussian, Inc., Pittsburgh, PA, 1998.

(37) Hay, P. J.; Wadt, W. R. *J. Chem. Phys.* **1985**, *82*, 299.

(38) Wadt, W. R.; Hay, P. J. *J. Chem. Phys.* **1985**, *82*, 285.

(39) Dunning, T. H., Jr.; Hay, P. J. In *Methods of Electronic Structure Theory*; Schaeffer, H. F., III, Ed.; Plenum Press: New York, 1977; p 1.

(40) Reed, A. E.; Curtiss, L. A.; Weinhold, F. *Chem. Rev.* **1988**, *88*, 899.

(41) Wolinski, K.; Hinton, J. F.; Pulay, P. *J. Am. Chem. Soc.* **1990**, *112*, 8251.

(42) Ruiz-Morales, Y.; Schreckenbach, G.; Ziegler, T. *J. Phys. Chem.* **1996**, *100*, 3359.

(23) Blöchl, P. E.; Togni, A. *Organometallics* **1996**, *15*, 4125.

(24) (a) Ward, T. R. *Organometallics* **1996**, *15*, 2836. (b) Gilardoni, F.; Weber, J.; Chermette, H.; Ward, T. R. *J. Phys. Chem. A* **1998**, *102*, 3607.

(25) Oslob, J. D.; Åkermark, B.; Helquist, P.; Norrby, P.-O. *Organometallics* **1997**, *16*, 3015.

(26) Aranyos, A.; Szabó, K. J.; Castaño, A. M.; Bäckvall, J.-E. *Organometallics* **1997**, *16*, 1058.

(27) Szabó, K. *Organometallics* **1996**, *15*, 1128.

(28) (a) Szabó, K. J. *J. Am. Chem. Soc.* **1996**, *118*, 7818. (b) Szabó, K. J. *Chem. Eur. J.* **1997**, *3*, 592. (c) Szabó, K. J. *Organometallics* **1997**, *16*, 3779. (d) Macsári, I.; Szabó, K. J. *Organometallics* **1999**, *18*, 701.

(29) Versluis, L.; Ziegler, T. *J. Chem. Phys.* **1988**, *88*, 322.

(30) (a) ADF version 2.3, Department of Theoretical Chemistry, Vrije Universiteit, Amsterdam. (b) Baerends, E. J.; Ellis, D. E.; Ros, P. *Chem. Phys.* **1973**, *2*, 41. (c) te Velde, G.; Baerends, E. J. *J. Comput. Phys.* **1992**, *99*, 84.

(31) Gunnarsson, O.; Lundquist, I. *Phys. Rev.* **1974**, *B10*, 1319.

(32) Vosko, S. H.; Wilk, L.; Nusair, M. *Can. J. Phys.* **1980**, *58*, 1200.

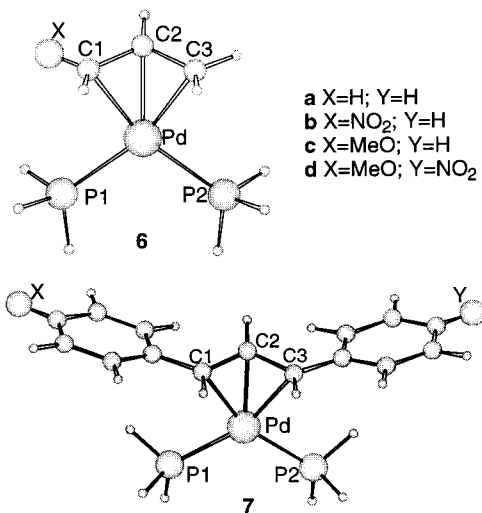


Figure 3. Structures of the model (η^3 -allyl)palladium and (η^3 -1,3-diarylallyl)palladium complexes **6a–c** and **7a–d**.

Table 1. Selected Geometry Parameters^a of the Model Allylpalladium Complexes 6 and 7

complex	Pd–C1	Pd–C2	Pd–C3	C1–C2	C2–C3	Pd–P1	Pd–P2
6a	2.19	2.19	2.19	1.40	1.40	2.30	2.30
6b	2.14	2.19	2.22	1.40	1.39	2.32	2.32
6c	2.32	2.19	2.15	1.40	1.41	2.33	2.32
7a	2.22	2.19	2.22	1.40	1.40	2.33	2.33
7b	2.22	2.19	2.23	1.40	1.40	2.31	2.32
7c	2.26	2.19	2.23	1.40	1.40	2.32	2.31
7d	2.25	2.17	2.19	1.40	1.40	2.32	2.31

^a See Figure 3 for compound designations. Bond lengths are given in Å.

Table 2. Charge Distribution^a in the Model Allylpalladium Complexes 6 and 7

complex	C1	C2	C3	allyl	Pd
6a	-0.44	-0.20	-0.44	-0.88	0.29
6b	-0.18	-0.45	-0.20	-1.01	0.30
6c	0.19	-0.47	-0.33	-0.77	0.24
7a	-0.24	-0.20	-0.24	-0.80	0.28
7b	-0.26	-0.20	-0.24	-0.84	0.26
7c	-0.25	-0.21	-0.23	-0.77	0.25
7d	-0.23	-0.21	-0.27	-0.80	0.26

^a Natural population analysis from the B3LYP densities obtained at the LDA geometries. Charges are given in au.

distances between Pd and the terminal carbon atoms of the allyl ligand (C1 and C3), while the Pd–C2 distance does not change significantly. In **6b** the Pd–C1 distance is shorter than the Pd–C3 one, while for **6c** the ordering between both distances is reversed. The comparison of both structures shows that the methoxy group induces more asymmetry than the nitro group.

For the (1,3-diphenylallyl)palladium complex **7a**, we can observe an increase of the Pd–C1 and Pd–C3 distances, with respect to the values obtained for **6a**. This result is a consequence of the larger steric requirements of the diphenylallyl ligand.

For the substituted (1,3-diarylallyl)palladium complexes **7b,c**, the values of the Pd–C1 and Pd–C3 distances present the same kind of asymmetry as for **6b,c**. The shortest Pd–C bond is the one involving the carbon atom closest to the most electron-withdrawing group. This asymmetry, however, is now less pronounced. Finally, for **7d** the substitution on both phenyl

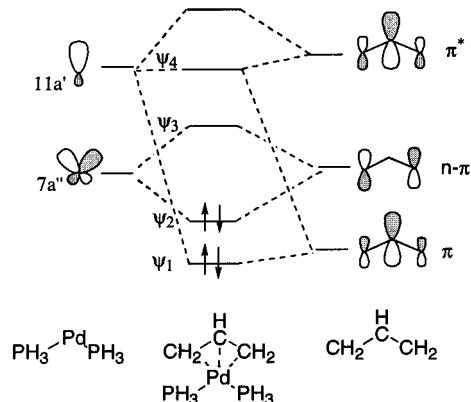


Figure 4. Schematic orbital interaction diagram for the (diphosphino)(η^3 -allyl)palladium complex **6a**.

groups induces a larger asymmetry in the Pd–C1 and Pd–C3 distances.

Table 2 presents charge distribution in the complexes **6** and **7**. We can observe that the allyl ligand has in all cases a negative charge, its magnitude depending on the nature of the substituents. This charge is larger in the complexes including the nitro group. Regarding the electron density on the allyl carbon atoms, we can see that in general terminal atoms are more negatively charged than C2. Nitro and methoxy groups directly bonded to C1 induce an important asymmetry in the charge distribution of the allyl ligand, while when these groups are linked through the phenyl groups the effect is less important. This asymmetry is especially important for **6c**, in which the charge on the C1 atom is positive.

To understand the effects induced by the substituents in the geometry of the complexes **6** and **7** and in the charge distribution we will analyze the Pd–allyl bond. In Figure 4 we present a schematic orbital interaction diagram for a (diphosphino)(allyl)palladium complex, **6a**. For the complexes containing symmetric allyl ligands, **6a** and **7a**, the interactions between the molecular orbitals of allyl and Pd(PH₃)₂ can be classified according to the two different symmetry species. The most important interaction in the metal–allyl bond is the one involving the $n-\pi$ orbital of the allyl fragment and the $7a''$ orbital of the metal fragment. This interaction involves two electrons, regardless of the way in which the electrons are partitioned between the fragments. There is a second interaction involving the occupied π orbital of the allyl ligand and the virtual $11a'$ orbital of Pd(PH₃)₂ with some mixing of the π^* orbital of the allyl moiety.

When one goes from the parent allyl fragment to the substituted ones, both the energy and the topology of the π orbitals change. Moreover, since the symmetry of the complex has been reduced, mixing between all π -allyl orbitals becomes possible. Figure 5 schematically represents the variation of these orbitals in the nitroallyl and methoxyallyl fragments. The presence of an electron-withdrawing group, such as a nitro group, lowers the energy of all these orbitals. Moreover, the $n-\pi$ orbital polarizes toward the nitro group. This orbital can be derived from the bonding combination between the $n-\pi$ orbital of the parent allyl anion and a low-lying empty orbital of the nitro group. The C–N bonding interaction is maximized through mixing with

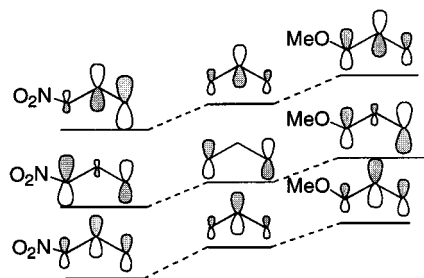


Figure 5. Effect of nitro and methoxy substituents bound to a terminal carbon atom upon the orbitals of the allyl moiety.

Table 3. ^{13}C NMR Chemical Shifts^a for the Model Complexes **7a–d**

	C1	C2	C3
7a	96.29 (90.10)	102.40 (111.60)	96.29 (90.10)
7b	93.10 (84.70)	104.06 (113.11)	97.27 (93.95)
7c	98.87 (91.45)	100.06 (110.32)	95.06 (88.90)
7d	100.52	99.65	89.37

^a In δ units relative to TMS. Experimental values corresponding to complexes **5**^{16b} are given in parentheses.

the allyl π^* orbital. The asymmetry in the coefficients in the C1 and C3 atoms in the $n-\pi$ orbital is consistent with the different values of the Pd–C bond lengths observed in Table 1. The variation of the orbital energies produces a diminution in the contribution of π in the bonding, while the contribution of π^* increases. This fact results in an increasing of the electron density in the allyl ligand with respect to **6a**, as can be observed in Table 2. When the substituent is an electron donor group, such as a methoxy group, the energies of the π orbitals increase. The contribution of the π orbital in the bonding becomes more important with respect to **6a** and the electron density on the allyl group decreases, as can be observed in Table 2. The methoxy group polarizes the $n-\pi$ orbital toward the C3 atom. This orbital can be derived from the antibonding interaction between the $n-\pi$ orbital of the parent allyl anion and a high-energy occupied orbital of the methoxy group. In this case the mixing with π^* minimizes the antibonding interaction between the methoxy group and the allyl terminal carbon atom. This fact is consistent with the asymmetry in the Pd–C bonds observed in Table 1.

For **7a** the presence of the phenyl groups produces a delocalization of the allyl π system. The presence of nitro and methoxy substituents has the same qualitative effect as for the simpler systems **6**, but this effect is quantitatively less important. These facts are consistent with the effect on the charge distribution (see Table 2) and with the values of the Pd–C bond lengths (see Table 1).

We have computed ^{13}C NMR chemical shifts for the allyl carbon atoms of the (1,3-diarylallyl)palladium complexes **7**, and the results obtained are presented in Table 3. We can observe that for **7a–c** the chemical shifts are downfield for the C2 atom in comparison to the shifts for the terminal C1 and C3 atoms, in good agreement with experiment. Regarding the substituted complexes **7b** and **7c**, our calculations qualitatively reproduce the observed differences in chemical shifts for

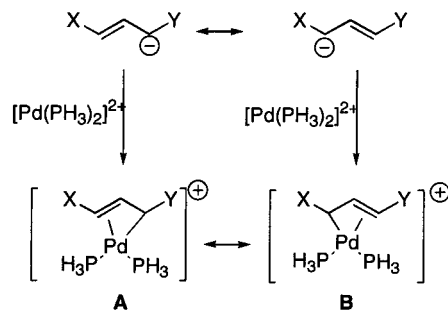


Figure 6. Resonance structures for disubstituted allyl anions and the corresponding allylpalladium cations.

C1 and C3 atoms. Finally, for **7d**, the effect of both substituents leads to a difference of more than 11 ppm between C1 and C3.

The differences between C1 and C3 chemical shifts in **7b–d** can have two different origins: the electronic effect of the substituents in the phenyl groups and the different values of the Pd–C bond lengths in the complexes. To analyze both effects, we have computed chemical shifts of **7b–d** by adding nitro and methoxy groups in the para position of the phenyl rings of **7a**, maintaining the geometry of **7a**. For **7b**, the $\Delta\delta(\text{C3}-\text{C1})$ value computed for the model geometry is 4.5 ppm, so that the electronic effect of the nitro group is clearly the origin of the asymmetry. On the other hand, for **7c**, $\Delta\delta(\text{C3}-\text{C1})$ computed for the model geometry is only -1.5 ppm. In this case, the difference in the real values of the Pd–C1 and Pd–C3 distances (see Table 1) also contribute to the final values of the chemical shifts. Finally, for the disubstituted complex **7d** $\Delta\delta(\text{C3}-\text{C1})$ is -6.0 ppm, so that the effect of both substituents is nearly additive.

An allylpalladium cation can be represented by the two resonance structures **A** and **B** shown in Figure 6. Each structure can be derived from the corresponding resonance structure of the allyl anion. In symmetrically disubstituted complexes, both structures would have the same weight, so that both terminal allyl carbon atoms have the same electronic environment. On the other hand, when X and Y are different, the electronic structure of the complex will be closer to one of the resonance structures. When X is a better electron donor group than Y, structure **A** is favored, while the reverse situation favors structure **B**. As a consequence, the allyl terminal carbon atom closer to the most electron-withdrawing group will have a greater sp^3 character than the other terminal carbon atom. The values of the Pd–C1 and Pd–C3 distances (Table 1) and of chemical shifts (Table 3) are in good agreement with this interpretation.

Let us now consider the nucleophilic attack at allylpalladium complexes. This process has been invoked to be determined by orbital interactions.^{21,43} In all the complexes studied, the LUMO is the antibonding combination of the $7a''$ orbital of $\text{Pd}(\text{PH}_3)_2$ and of the $n-\pi$ orbital of the allyl moiety (Ψ_3 in Figure 4), so that the attack would take place with preference at the C1 and C3 atoms.

(43) (a) Schilling, B. E. R.; Hoffmann, R.; Faller, J. W. *J. Am. Chem. Soc.* **1979**, *101*, 592. (b) Curtis, M. D.; Eisenstein, O. *Organometallics* **1984**, *3*, 887.

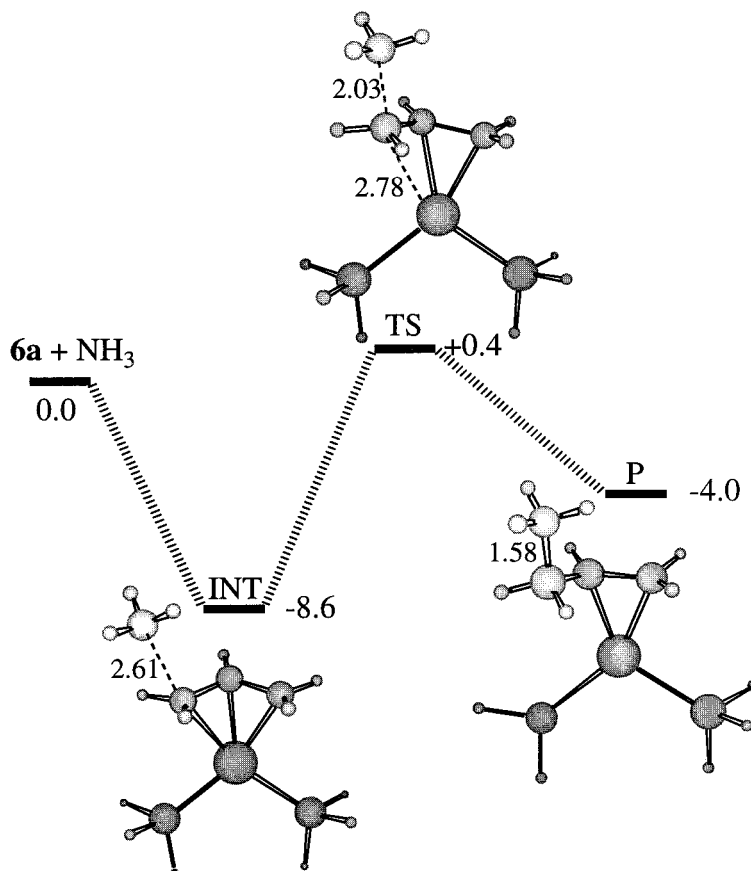


Figure 7. Schematic energy profile for ammonia attack at one of the allyl terminal carbon atoms of **6a** obtained at the B3LYP level of calculation. Relative energies are in kcal mol⁻¹, and selected bond distances are in Å.

The examination of the LUMO coefficients on these carbon atoms does not allow us to predict the regioselectivity of the attack. We have observed that the largest LUMO coefficient is in the carbon atom linked to the most electron-withdrawing aryl group and is closer to Pd, while experiments indicate that this is not the site preferred for nucleophilic attack. To understand the observed regioselectivity, one should consider the interaction of the allylpalladium complexes with a nucleophile attacking the different sites.

The reaction between an allylpalladium cationic complex and a negatively charged nucleophile is expected to take place without any barrier in the gas phase, while in solution there would be a barrier associated with the desolvation of both reactants.⁴⁴ The theoretical treatment of such a process would require a realistic modeling of the solvent. Unfortunately, the size of the allylpalladium complexes **7b–d** precludes this kind of calculation with our present computational resources.

Relevant information about the nucleophilic attack can be obtained using a neutral nucleophile such as ammonia.²³ We have studied the attack of an ammonia molecule at one of the terminal carbon atoms of **6a** using the B3LYP method, and we have located the stationary points shown in Figure 7. This process leads to the formation of an η^2 -olefin complex previous to final products.^{2b} The formation of such complexes has been spectroscopically detected recently by Helmchen and co-

workers.⁴⁵ More recently, Kuhn and Mayr⁴⁶ have also postulated the formation of this type of complex in the reactions of neutral nucleophiles with (phenylallyl)-palladium cations.

Figure 7 shows that the reaction between **6a** and ammonia takes place through the formation of an intermediate (INT) at large C–N distances. This process does not require any energy barrier. The transition state (TS) leading to the formation of the η^2 -olefin complex (P) is placed 9 kcal mol⁻¹ above the intermediate, with a C–N bond distance at the transition state (2.03 Å) in excellent agreement with values reported for intramolecular processes.⁴⁷

For the nucleophilic attack of ammonia at complexes **7b–d** we have optimized the geometries of the intermediates and of the η^2 -olefin complexes. Regarding the transition states, we have considered structures with the ammonia molecule 2 Å away from one of the allyl terminal carbon atoms. This distance, which corresponds to the distance obtained for the transition state of the reaction of **6a**, has been kept frozen, and all the remaining geometry parameters have been optimized. The results obtained in this study are presented in Table 4.

We can observe that for the intermediates at large C–N distance there is no preference for the interaction with either of the two allyl terminal carbon atoms. On

(45) Steinhagen, H.; Reggelin, M.; Helmchen, G. *Angew. Chem., Int. Ed. Engl.* **1997**, *36*, 2108.

(46) Kuhn, O.; Mayr, H. *Angew. Chem., Int. Ed.* **1999**, *38*, 343.

(47) (a) Sakaki, S.; Satoh, H.; Shono, H.; Ujino, Y. *Organometallics* **1996**, *15*, 1713. (b) Szabó, K. *Organometallics* **1998**, *17*, 1677.

(44) Dewar, M. J. S.; Storch, D. M. *J. Chem. Soc., Perkin Trans 2* **1989**, 877.

Table 4. Energy^a Relative to Isolated Fragments for Stationary Points of the Reaction Coordinate Corresponding to Nucleophilic Attack of NH₃ at the C1 and C3 Atoms of 7b–c

	stationary point ^b	C1	C3
7b	INT	-2.9	-2.9
	TS	8.9	5.3
	P	7.8	3.8
7c	INT	-1.8	-1.8
	TS	8.2	11.3
	P	8.4	11.0
7d	INT	-3.2	-3.1
	TS	4.9	9.9
	P	4.7	11.4

^a In kcal mol⁻¹. ^b See Figure 7.

Table 5. Selected Geometry Parameters^a for Transition States Corresponding to the Attack of an Ammonia Molecule at One of the Allyl Terminal Carbon Atoms of the Model Complexes 7b–d

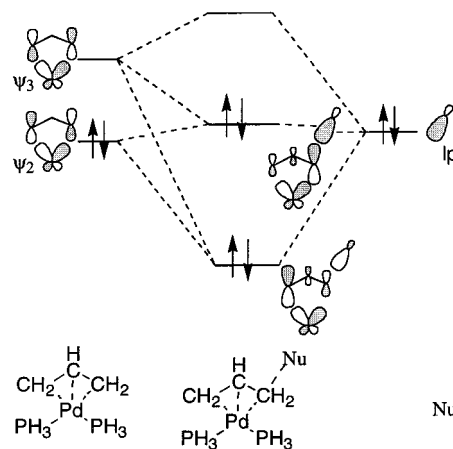
	attack	Pd–C1	Pd–C2	Pd–C3
7b	C1	2.65	2.16	2.16
	C3	2.15	2.15	2.70
7c	C1	2.75	2.15	2.14
	C3	2.16	2.15	2.62
7d	C1	2.77	2.14	2.14
	C3	2.17	2.16	2.64

^a Bond lengths in Å.

the other hand, Table 4 shows that in all cases the most favorable transition state and the most stable η^2 complex are the ones in which the nucleophile attacks the allyl carbon atom closer to the most electron-donating group, in excellent agreement with the experimentally observed regioselectivity.¹⁶ The fact that at long C–Nu distances there is no preference for any of the two possible sites of attack, while at intermediate and short distances a significant preference for one of the sites is observed, would be consistent with a late transition state in the process.^{2b,45}

The optimized values of the Pd–C distances at the transition states are shown in Table 5. If we compare these values with the ones corresponding to the isolated complexes for these structures (Table 1), we can observe that, in all cases, the Pd–C bond distance corresponding to the attacked allyl carbon atom increases, so that this bond is partially broken. When the nucleophile attacks the carbon atom with the longest Pd–C bond (C3 for **7b** and C1 for **7c** and **7d**), the increasing of the Pd–C distance is larger than when the attack takes place at the other site.

To aid in an understanding of the origin of the regioselectivity, Figure 8 shows a schematic orbital interaction diagram between the allylpalladium complex **6a** and the nucleophile. The most important interaction between the incoming nucleophile and the complex is

**Figure 8.** Schematic orbital interaction diagram between the (diphosphino)(η^3 -allyl)palladium complex **6a** and the nucleophile.

the one involving the lone pair (lp) of the nucleophile and the LUMO of the complex (Ψ_3). The bonding combination of these two orbitals has a Pd–allyl antibonding character. Mixing with the remaining orbitals of the allylpalladium complex, especially with Ψ_2 , polarizes this orbital in such a way that the Pd–C repulsive interaction is maximized for the allyl carbon atom attacked by the nucleophile, while it is minimized for the other allyl terminal carbon atom. This interaction would lead to an increasing of the Pd–C distance corresponding to the attacked carbon atom and to a shortening of the other terminal Pd–C bond, as observed in Table 5. For asymmetric allyl ligands this polarization would favor attack at the allyl terminal carbon atom with the longest Pd–C bond in order to minimize the Pd–C antibonding interaction.

The energy barriers for the nucleophilic attack shown in Table 4 can be analyzed in terms of two contributions: the distortion energy of the reactants (ΔE_{dist}) and the interaction energy between both distorted fragments (ΔE_{int}). This term would include both repulsive and attractive contributions. The results obtained in this analysis are shown in Table 6. In all cases the energy barrier mainly arises from the distortion of the reactants, while the interaction energy term is stabilizing, so that the attractive interactions between ammonia and the allylpalladium cation overcome the repulsive ones. Regarding the differences between energy barriers corresponding to the attack to C1 and C3, we can observe that for **7b** the regioselectivity is mainly determined by the interaction energy term. This is consistent with the polarization mechanism discussed above (see Figure 8). Moreover, the distortion energy term slightly favors the attack to C3. This result can be related to the variation of the Pd–C bond lengths on going from the equilibrium geometry to the transition state. The

Table 6. Analysis of the Energy Barriers^a for the Nucleophilic Attack of Ammonia at One of the Terminal Allyl Carbon Atoms of Complexes 7b–d

	7b		7c		7d	
	C1	C3	C1	C3	C1	C3
ΔE_{dist}	14.2 (+0.9)	13.3 (0.0)	12.3 (0.0)	15.0 (+2.7)	11.0 (0.0)	13.6 (+2.6)
ΔE_{int}	-5.3 (+2.7)	-8.0 (0.0)	-4.1 (0.0)	-3.7 (+0.4)	-6.1 (0.0)	-3.7 (+2.4)
ΔE	8.9 (+3.6)	5.3 (0.0)	8.2 (0.0)	+11.3 (+3.1)	4.9 (0.0)	9.9 (+5.0)

^a In kcal mol⁻¹. See text for definitions. In parentheses are given values relative to the most favorable structure.

comparison of Tables 1 and 5 shows that for **7b** the Pd–C1 distance increases by 0.43 Å when the nucleophile attacks C1, while for the attack at C3 the lengthening of the Pd–C3 distance is 0.47 Å.

With regard to **7c**, Table 6 shows that the main contribution to the regioselectivity comes from the distortion energy term. There is also a smaller contribution of the interaction term, which is consistent with the minor contribution of the allyl π^* orbital in the Pd–allyl bonding in the methoxy complexes compared to nitro complexes discussed above (see Figures 4 and 5). The larger difference in the distortion energy term for the attack at C1 and C3 is due to the different degrees of geometry distortion of the (diarylallyl)palladium fragment. For the attack at C1, the Pd–C1 distance increases by 0.49 Å with respect to the isolated complex (see Tables 1 and 5), while for the attack at C3 the increase of the Pd–C3 distance is 0.39 Å.

In the preceding discussion we have shown that two factors seem to determine the regioselectivity for the nucleophilic attack at allylpalladium cations. First, the distortion energy of the allylpalladium fragment is lower when the attack takes place at the allyl terminal carbon atom with the longest Pd–C distance. This factor seems to be the dominant one for **7c**. The second factor is the interaction energy between distorted allylpalladium and nucleophile fragments that also favors the attack at the allyl terminal carbon with the longest Pd–C bond. This factor seems to be the most important for **7b**. Finally, Table 6 shows that, for **7d**, the contributions of both factors to the regioselectivity are similar.

Conclusion

The geometries of several mono- and disubstituted (diphosphino)(η^3 -allyl)palladium cations have been optimized using density functional methods. The results obtained show that for unsymmetrical allyl ligands the

shortest Pd–C(terminal) bond is the one closest to the most electron-withdrawing group. This fact has been rationalized in terms of molecular orbital interactions between the allyl ligand and the metal. The computed ^{13}C NMR chemical shifts for the allyl carbon atoms in the 1,3-diarylallyl complexes **7a–c** show that the central carbon atom, C2, is always less shielded than the terminal carbon atoms, C1 and C3. We have discussed the origin of chemical shift differences between allyl terminal carbon atoms (electronic effects and Pd–C bond lengths). For the substituted complexes **7b,c**, the carbon atom closest to the most electron-donating group presents an downfield chemical shift, in excellent agreement with experimental observations. Experimental results show that nucleophilic attack takes place at this carbon atom, which presents a longer Pd–C bond.

The nucleophilic attack of ammonia at allylpalladium complexes **6a** and **7b–d** has been studied. For the unsymmetrically substituted complexes **7b–d** the results obtained predict that the attack would take place preferentially at the allyl terminal carbon atom closest to the most electron-donating substituent (C3 for **7b** and C1 for **7c** and **7d**), in excellent agreement with experiments. This regioselectivity has been rationalized in terms of molecular orbital interactions and by considering the geometry distortion induced by the interaction with the nucleophile at the transition state.

Acknowledgment. Financial support from the DGI-CYT (MEC of Spain) through project PB93-0896, and from the CIRIT (Generalitat de Catalunya) through project 96SGR-0030, a predoctoral scholarship (to F.P.), and computer time from the “Centre de Supercomputació de Catalunya” (CESCA) are gratefully acknowledged. We also thank Prof. Per-Ola Norrby for communicating results prior to publication.

OM990371S